Journal of Applied Electrochemistry **34**:1271–1278, 2004.

Electrodeposition of magnesium from the eutectic LiCl–KCl melt

A.M. MARTÍNEZ[1,*], B. BØRRESEN[1], G.M. HAARBERG[1], Y. CASTRILLEJO[2] and R. TUNOLD[1]
[1]*Department of Materials Technology, Norwegian University of Science and Technology, Sem Saelands vei 6, 7491-Trondheim, Norway*
[2] *Departamento de Química Analítica, Facultad de Ciencias, Universidad de Valladolid, Prado de la Magdalena s/n, 47005-Valladolid, Spain*
*(*author for correspondence, e-mail: martinez@material.ntnu.no)*

Received 6 January 2004; accepted in revised form 14 July 2004

Key words: electrochemistry, electrodeposition, magnesium, molten chlorides, nucleation

Abstract

Electrodeposition of magnesium in the eutectic LiCl–KCl mixture (58–42 mol%) containing different $MgCl_2$ concentrations was studied using tungsten as cathode material. The temperature was varied above and below the melting point of magnesium (983 K). Electrochemical techniques such as cyclic voltammetry, chronopotentiometry and chronoamperometry were employed in order to characterise the system and study nucleation and growth of the magnesium phase. With all the electrochemical techniques above mentioned, macroscopic growth of the solid magnesium deposit was observed. Liquid magnesium deposits were found to grow without giving rise to a significant increase in surface area. This may be related to lithium co-deposition and formation of Li–Mg liquid solution and the differences in interfacial properties of the cathodic deposits obtained in each case. The deposition of lithium on pre-deposited magnesium leads to the formation of Li–Mg solid alloys or to a liquid Li–Mg solution at temperatures below or above the melting point of magnesium, respectively. The diffusion coefficient of magnesium ions was determined by different electrochemical techniques. The values obtained showed the effect of macroscopic growth of the deposit in the case of solid magnesium deposits.

1. Introduction

Despite the many recent improvements in thermal methods, electrolysis is still the main technique for industrial production of magnesium. Electrolytic production of magnesium in molten chlorides is an energy demanding process [1–3], hence optimisation with respect to current and energy efficiencies is necessary in order to achieve cost competitive production. For this reason, studies of the effect of some of the main causes of losses in current efficiency have been carried out.

The current efficiency of the electrolytic process depends critically on the purity of the feed material, in this case the quality of the anhydrous magnesium chloride feed, and it is typically in the range 85–90%.

Good wetting of the cathode by magnesium is also important. Otherwise fine droplets of magnesium will be formed which easily recombine with chlorine by recirculation and long residence time in the electrolyte. Steel cathodes are employed due to their stability, but they have poor wetting properties and, in addition, the magnesium produced will be contaminated by iron due to corrosion. Research on alternative cathode materials is hence needed.

Different electrolytic methods can be distinguished depending, among other things, on the cell feed (raw material and preparation of magnesium chloride). In practice, the composition of the electrolyte is chosen according to the raw material [3]. If the electrolysers are fed with magnesium chloride, the electrolyte may contain, as well as $CaCl_2$, $BaCl_2$ and LiCl, NaCl and KCl (as in the case of carnallite feed), depending on the composition of the starting material and its preparation for the dehydration. In particular LiCl has always been very interesting to investigate as a component of the electrolyte because of the existence of large reserves of native magnesium chloride brines containing major amounts of lithium chloride that may build up in the electrolyte. There have been several published papers on the electrochemistry of magnesium ions in the molten eutectic LiCl–KCl mixture. However, such studies have not dealt with the nucleation and crystallisation of magnesium on foreign substrates.

Furihata et al. [4, 5] reported results obtained in a LiCl–KCl–$MgCl_2$ mixture at 450 °C using a platinum microelectrode. They found that the equilibrium potential of Mg(II)/Mg is very close to the discharge potential of lithium or potassium ions, as previously reported [6].

The authors also studied the influence of moisture in the electrochemical system by adding $MgCl_2$ hexahydrate to the purified molten chloride. In this case they reported a significant residual cathodic current, and it was impossible to obtain a clear Mg(II) reduction wave.

Several authors have also studied the electrochemical behaviour of Li–Mg alloys in a LiCl–KCl electrolyte [7, 8], which is of interest in lithium rechargeable batteries. They found that the discharge and solution processes of Li–Mg alloys in these melts are diffusion controlled.

A study by Le Vaguerese [9] reports the properties of $MgCl_2$ solutions in various molten chlorides, among them LiCl–KCl, in various pyrochemical processes for treatment of nuclear fuels. The author reported problems related to the presence of OH^- in the LiCl–KCl solvent, probable due to the hygroscopic nature of LiCl and $MgCl_2$ and the lack of purification of the molten chloride.

More recently Støre et al. [10] studied the electrochemical reduction of Mg(II) ions at glassy carbon and tungsten electrodes in the eutectic LiCl–KCl mixture. The authors determined the diffusion coefficient of magnesium ions by different electrochemical techniques, i.e., cyclic voltammetry, convolution analysis and chronopotentiometry, and its variation with the temperature in the range 375–500 °C.

Due to the importance of the presence of oxide ions in the lithium chloride-based melts, several studies have been devoted to the possibility of measuring the amount of O^{2-} ions in the bath by means of a zirconia-stabilised membrane electrode [11, 12].

In addition to the electrochemical studies, Bukun and Ukshe [13] reported the values of solubility of metallic magnesium in several fused chlorides, among them single LiCl. The authors found that solubility of magnesium in the melt depends on the temperature, electrolyte composition and activity of magnesium chloride. They also discussed possible structures for the magnesium subhalide ions, suggesting that the most probable mechanism of dissolution is the establishment of the equilibrium:

$$Mg + MgCl_2 \Leftrightarrow 2MgCl \quad (1)$$

However, later studies carried out by Van Norman and Egan [14] showed that the dissolution of magnesium in its chloride most likely follows the equilibrium:

$$Mg + MgCl_2 \Leftrightarrow Mg_2Cl_2 \quad (2)$$

This paper is part of a series of systematic studies carried out in order to elucidate the different and complicated phenomena that take place during magnesium electrodeposition from chloride melts. The understanding of these processes may facilitate appropriate choice of the electrode material and melt compositions and could hence help in the optimisation of the industrial process of magnesium production.

2. Experimental

The experiments were carried out inside a glove box (VAC Model HE-43-2) in an inert argon atmosphere. The moisture and oxygen levels inside the box were kept below 1 ppm. The equimolar LiCl–KCl mixture (58–42 mol%) containing different $MgCl_2$ amounts (0.5 and 2 mol%), was melted in a glassy carbon crucible (Carbone Lorraine) placed in a quartz cell inside a furnace. A Eurotherm Model 2404 programmable device controlled the temperature of the furnace (± 2 °C), which was measured with a thermocouple (Pt/Pt–Rh 10%) protected by an alumina tube inserted into the melt. The working temperatures were 673, 823 and 1000 K.

The working electrode was a 1 mm tungsten wire (Alfa, 99.995%). A 3 mm glassy carbon rod (Tokai Carbon Co. grade GC-20S), the glassy carbon crucible or a magnesium electrode, were used as counter electrode. The reference electrode consisted of a solid magnesium rod or magnesium pool (Riedel-De Haen, 99.8%), depending on the working temperature. All potentials are referred to the Mg(II)/Mg system.

The lower ends of the tungsten electrodes were polished thoroughly by using SiC paper and 1 μm diamond paste. Then they were cleaned in ethanol using ultrasound followed by heating under high vacuum.

Purification of the LiCl and KCl salts (p.a. grade) consisted of heating the salt up to ca. 600 °C under vacuum. Dehydrated $MgCl_2$ was prepared from commercial $MgCl_2{\cdot}6H_2O$, by drying it carefully under HCl atmosphere. The dried $MgCl_2$ was subsequently distilled under vacuum [15]. The pure salts were stored and handled inside the glove box.

3. Results and discussions

3.1. *Dilute $MgCl_2$ solutions in the equimolar LiCl–KCl melt*

Typical voltammograms obtained on a tungsten electrode in the eutectic LiCl–KCl at 673 K containing a dilute solution of $MgCl_2$ (0.084 mol kg^{-1} or 0.5 mol%), are shown in Figure 1(a) and 1(b).

The electrochemical reduction of Mg(II) species takes place in a single step characterised by the cathodic wave B, associated with the reoxidation peak B′. The shape of B/B′ is characteristic of the formation of a product that remains adhered to the electrode and is related to the Mg(II)/Mg(solid) electrochemical exchange.

The formation of a deposit has been confirmed by examination of voltammograms. When analysing the system B/B′ separately, the ratio of the anodic to cathodic current is greater than unity and the ratio of the total anodic to the total cathodic charge is close to unity and independent of the scan rate.

According to the phase diagram of the Li/Mg system (see Figure 2), D/D′ waves probably correspond to the

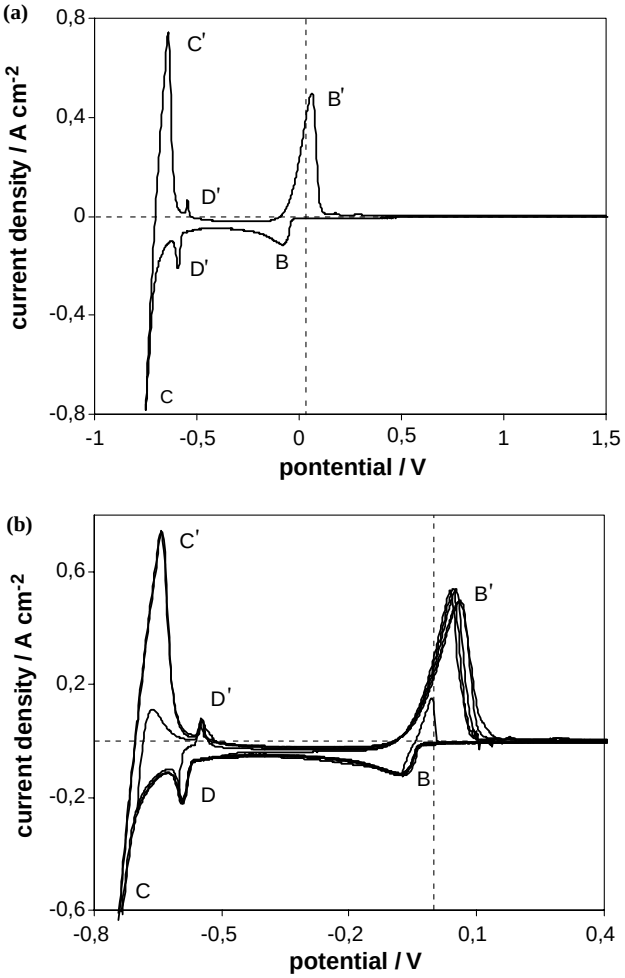

Fig. 1. (a) Voltammogram obtained in molten eutectic LiCl–KCl mixture at 673 K containing 0.5 mol% $MgCl_2$. $v = 0.2\ V\ s^{-1}$ (b) Voltammograms obtained at different cathodic limits. The conditions are the same as in (a).

formation of a Li–Mg solid alloy [16] by underpotential deposition of lithium on the solid magnesium deposit already covering the tungsten electrode. The cathodic limit of the melt (C/C′ system) corresponds to deposition of liquid lithium and subsequent reoxidation.

Despite the presence of potassium chloride, which has the effect of increasing the interfacial tension between the melt and the substrate [3], there was no evidence of monolayer formation of magnesium on tungsten electrodes in the eutectic LiCl–KCl mixture, contrary to what was found in $CaCl_2$–NaCl–KCl–$MgCl_2$ melts [17]. It is likely that the effect of lithium chloride on the interfacial properties is stronger than the effect of KCl, so in this type of melt formation of three-dimensional magnesium deposits is more favoured than the formation of two-dimensional magnesium layers. This could explain the absence of any current peak corresponding to a Mg monolayer formation. Voltammograms obtained at 823 K showed similar features (see Figure 3). However, when increasing temperature to 1000 K, voltammetric curves showed a pronounced UPD of lithium on the liquid magnesium already deposited on the tungsten substrate (see Figures 3 and 4), due to the higher solubility of liquid lithium in the liquid magnesium at higher temperatures [16]. The fact that peak C′ is now less sharp may be due to three reasons:

- Increased solubility of lithium in the molten chloride when increasing the temperature.
- Increased solubility of lithium in magnesium and subsequent oxidation of soluble lithium from Li–Mg solution

It was possible to calculate the diffusion coefficient of Mg(II) ions from data obtained by cyclic voltammetry and associated techniques (i.e., convolution of the

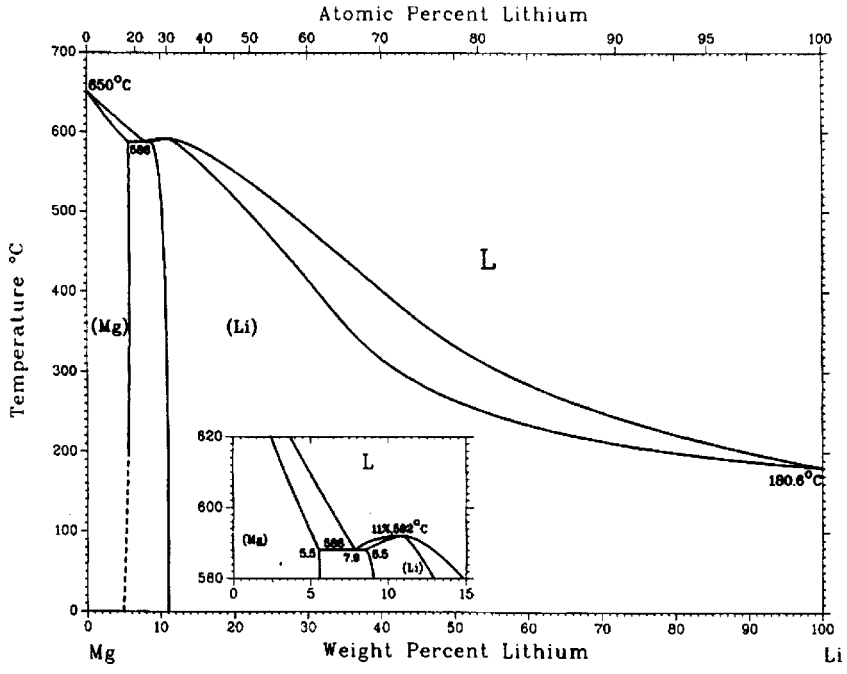

Fig. 2. Phase diagram of the Mg/Li system [16].

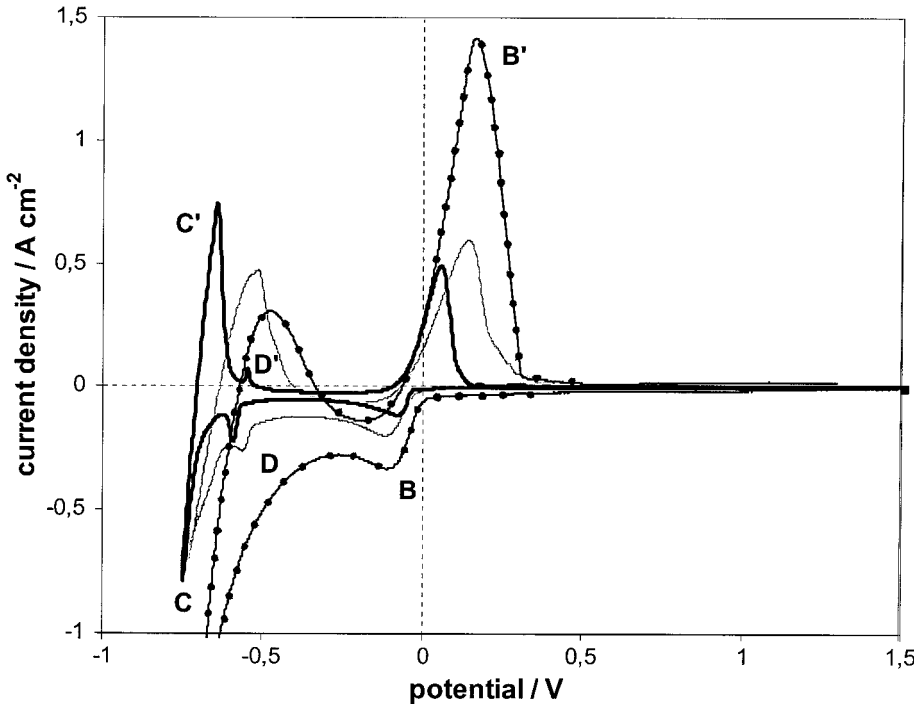

Fig. 3. Voltammograms obtained in the eutectic LiCl–KCl mixture containing a dilute $MgCl_2$ solution (≈0.5 mol%) at different temperatures (—) T = 673 K; (—) T = 823 K; (–●–●–) T = 1000 K.

voltammetric curves), by applying Berzins–Delahay equation in the case of voltammetry:

$$I_{pc} = 0.61(nF)^{3/2}(RT)^{-1/2}AC_oD^{1/2}\tilde{o}^{1/2} \quad (3)$$

where I_{pc} is the cathodic peak current of the B/B′ system, C_o the bulk concentration of the electroactive species, D the diffusion coefficient and A the electrode surface area.

In the case of the convolution technique, Equation 4 is applied:

$$m^* = nFAC_oD^{1/2} \quad (4)$$

where m^* is the maximum value reached for the convoluted current of the voltammograms. An example of a voltametric curve and its corresponding convoluted curve is shown in Figure 5.

The results are gathered in Table 1. Values extracted from cyclic voltammetry are generally lower than those obtained by convolution. This may be due to the effect of growth of the deposit which increases the electroactive area of the cathode. Another possible explanation may be the effect of lithium co-deposition. This affects the results obtained by convolution of the voltammetric curves since this technique utilises data recorded at longer time frames.

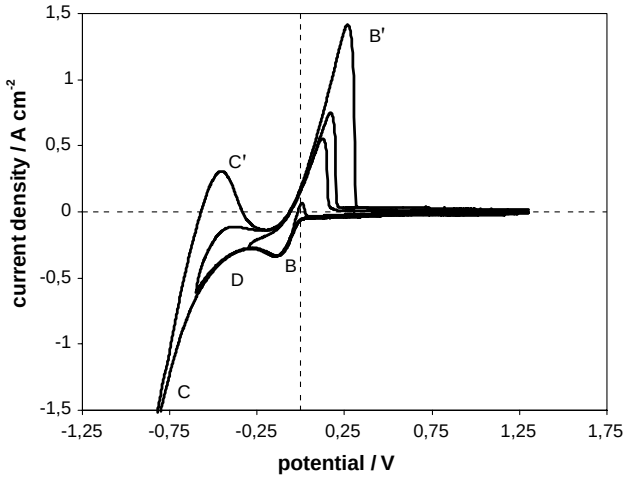

Fig. 4. Voltammograms obtained in molten eutectic LiCl–KCl mixture at 1000 K containing 0.5 mol% $MgCl_2$ v = 0.2 V s^{-1}.

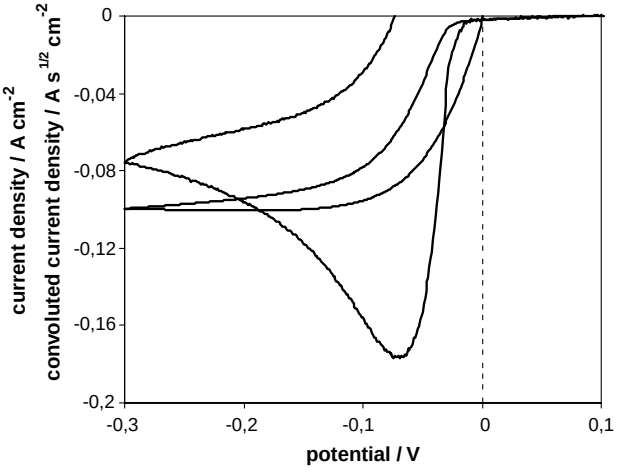

Fig. 5. Example of voltammogram and corresponding convoluted curve. Molten eutectic LiCl–KCl mixture at 673 K containing 0.5 mol% $MgCl_2$ v = 0.4 V s^{-1}.

Table 1. Diffusion coefficient (D $10^5/cm^2\ s^{-1}$) of Mg(II) species obtained by different electrochemical techniques in the molten eutectic LiCl–KCl mixture at different temperatures

Technique	T = 673 K	T = 823 K	T = 1000 K
Cyclic voltammetry	0.8	1.7	2.1
Convolution analysis	1.2	3.8	5.2
Chronopotentiometry	1.7	2.3	–
Chronoamperometry	1.2	3.1	5.6

Chronoamperometric curves obtained at temperatures below the melting point of metallic magnesium (see Figure 6) were characteristic of growth of the deposit (increase in electroactive area) at applied potentials more cathodic than −0.200 V. However, at a working temperature of 1000 K, the transients showed typical features of a reduction process controlled by planar diffusion (see Figure 7). This could indicate that the deposit has different morphologies in the two cases. Due to the increase in UPD of lithium at higher temperatures, a lithium–magnesium alloy is formed almost from the beginning of the formation of the magnesium phase on the tungsten substrate. The results also indicate the different interfacial properties of the magnesium metal vs the Mg–Li alloy. In the case of solid magnesium a dendritic deposit is formed. However, when depositing liquid magnesium, lithium is co-deposited at more positive potentials causing a lithium–magnesium liquid solution being uniform in shape (better coalescence).

3.2. *Effect of increased $MgCl_2$ concentration (2 mol%)*

Figure 8 shows a typical voltammogram obtained in the equimolar LiCl–KCl mixture containing 2 mol% $MgCl_2$ at 823 K. A more pronounced UPD of lithium is observed from the figure and it is due to an increase in the lithium chloride activity [18]. The increased activity is probably related to the ability of $MgCl_2$ to form complexes with KCl (K_2MgCl_4). Moreover lithium co-

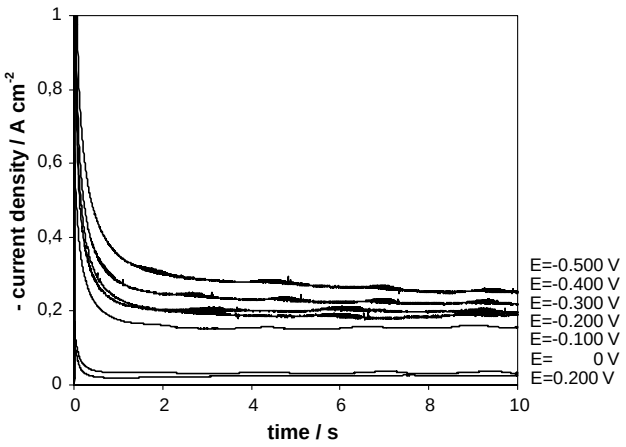

Fig. 7. Current transients obtained in eutectic LiCl–KCl mixture containing $MgCl_2$ (0.75 mol%) at 1000 K. Applied potentials vs Mg reference electrode.

deposition can be seen in the 'shoulder', D″, of the reoxidation peak B′, which appears even when the vertex potential is not very cathodic.

Furthermore, the potential window between Mg and Li deposition is reduced (compare Figures 3 and 8) and the solubility of lithium metal in the molten chloride increases as a consequence of the increased LiCl activity.

The group of anodic current spikes, E′, is probably related to the oxidation of lithium droplets. Similar features have also been observed when oxidising magnesium droplets in the pure $MgCl_2$ melt [15, 19].

Moreover the cross-over in the cathodic region is probably due to the effect of macroscopic growth of the deposit (increase in electrode area).

Chronopotentiometric curves obtained in the equimolar LiCl–KCl mixture containing 2 mol% $MgCl_2$ at 823 K are shown in Figure 9. The potential is initially determined by the Mg(II)/Mg(solid) system and it gradually becomes more negative due to depletion of Mg(II) species in the vicinity of the electrode. When the concentration of Mg(II) drops to zero, there is a sudden

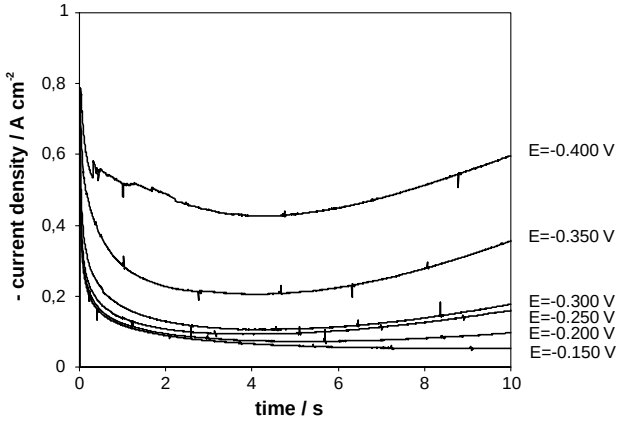

Fig. 6. Current transients obtained in eutectic LiCl–KCl mixture containing $MgCl_2$ (0.5 mol%) at 673 K. Applied potentials vs Mg reference electrode.

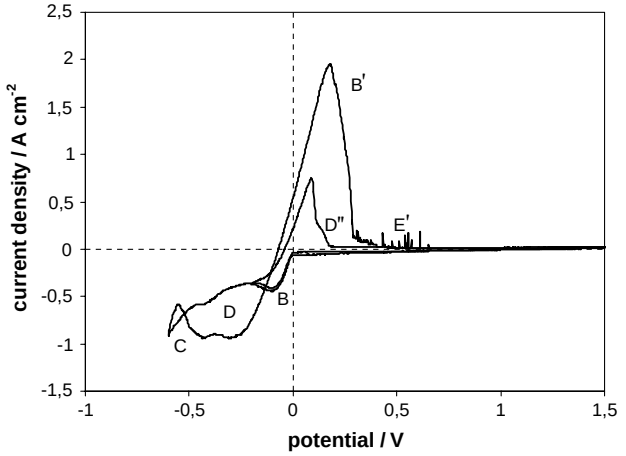

Fig. 8. Voltammograms obtained in molten eutectic LiCl–KCl mixture at 823 K containing 2 mol% $MgCl_2$ v = 0.2 V s^{-1}.

potential increase, and the potential is not reaching the reduction potential of the lithium ions, or the potential for Li–Mg alloy formation, but becomes more positive. This decrease in over voltage could be due to the growth of the deposit, which increases the electrode area hence decreasing the current density. Nucleation and growth of the solid magnesium deposit are also evidenced by chronoamperometric curves. Figure 10(a) shows the increase in cathodic current with time, due to the increase in electrode area. It is probable that at the higher over potentials some lithium is co-deposited, which could also be the reason for the instability in the current. Plots of the current vs $t^{1/2}$ at different applied potentials (Figure 10(b)) indicate instantaneous nucleation of the solid magnesium deposit.

As was shown in the case of low $MgCl_2$ content (Figure 7), the effect of the growth of the magnesium deposit is not indicated at higher $MgCl_2$ content (2 mol%) when forming liquid Mg. This is observed in the voltammetric, chronopotentiometric and chronoamperometric curves obtained.

Figure 11 shows typical cyclic voltammograms obtained in the equimolar LiCl–KCl mixture containing 2 mol% $MgCl_2$ at 1000 K. Comparing Figure 11 and Figure 8, a more pronounced UPD of lithium on the liquid magnesium already deposited on the tungsten substrate forming a liquid Li–Mg solution is seen [16]. It is likely that lithium co-deposition is playing an important role in the growth of the cathodic deposit. Electrodeposition of lithium to form Li–Mg alloy changes the interfacial properties such that the cathodic deposit coalesces more easily. As is well known, the 'shape' of a growing deposit often is determined by surface chemical factors [20].

Absence of growth of the cathodic deposit above the melting point of magnesium can also be demonstrated by chronopotentiometry (Figure 12) and chronoamperometry (Figure 13).

Chronopotentiometric curves showed expected features: first reduction of Mg(II) and then, when Mg(II) is depleted from the electrode interface, reduction of Li(I) ions. Chronoamperometric curves only showed a slight increase in cathodic current at a very high over potential (−0.500 V) where it is most likely that lithium is co-deposited. The spikes in the curve obtained at the

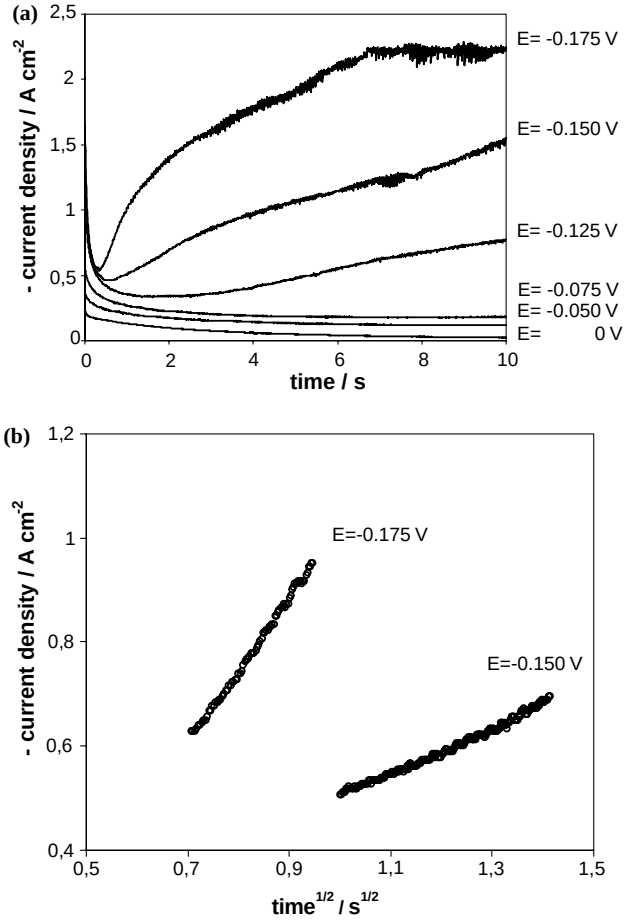

Fig. 10. (a) Chronoamperograms obtained in molten eutectic LiCl–KCl mixture at 823 K containing 2 mol% $MgCl_2$. Applied potentials vs Mg reference electrode. (b) I vs $t^{1/2}$ plots showing instantaneous nucleation.

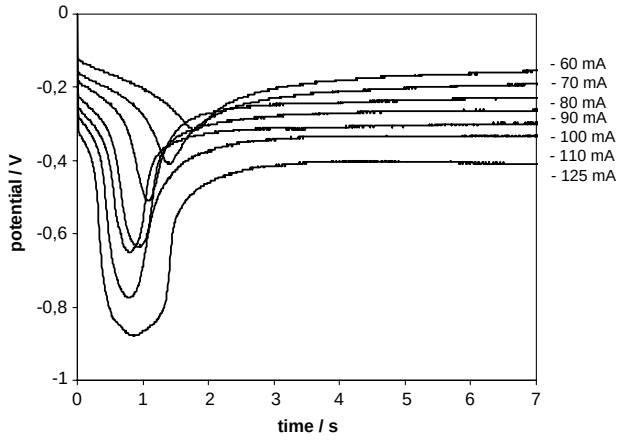

Fig. 9. Chronopotentiograms of the molten eutectic LiCl–KCl mixture at 823 K containing 2 mol% $MgCl_2$ Electroactive area A = 0.18 cm^2.

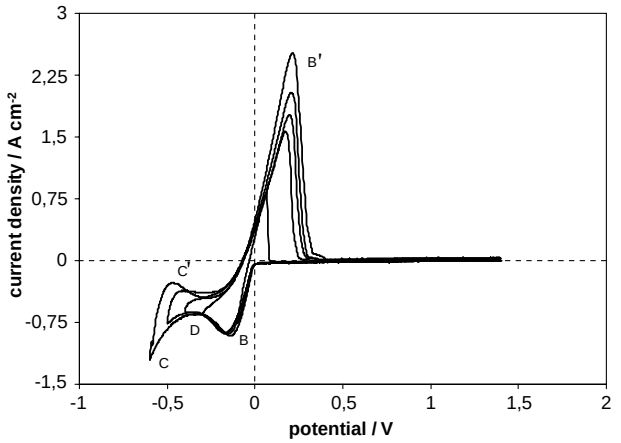

Fig. 11. Cyclic voltammograms obtained in molten eutectic LiCl–KCl mixture at 1000 K containing 2 mol% $MgCl_2$ v = 0.2 V s^{-1}.

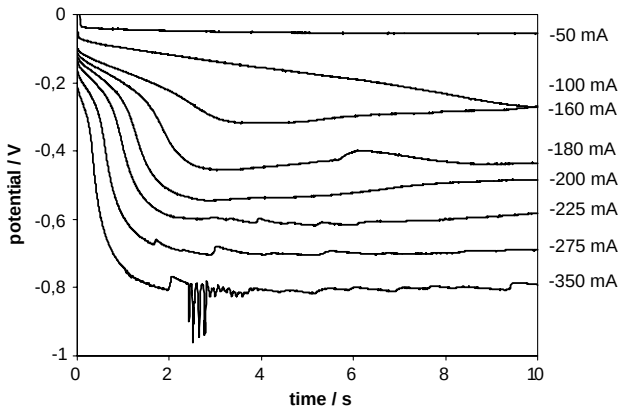

Fig. 12. Chronopotentiograms obtained in molten eutectic LiCl–KCl mixture at 1000 K containing 2 mol% $MgCl_2$ Electroactive area A = 0.16 cm^2.

most negative potential (i.e., −0.500 V) are probably due to formation and detachment of lithium droplets, which presence was also indicated in Figure 8 (anodic current spikes E′).

4. Conclusions

UPD of Li on the Mg already deposited on the tungsten electrode due to Mg–Li alloy formation is probably the most remarkable effect in this type of melt. This UPD is more pronounced when increasing the working temperature and the $MgCl_2$ content in the equimolar LiCl–KCl mixture. It is likely that lithium co-deposition cannot be avoided due to the proximity of the standard potential of the Mg(II)/Mg(0) couple to the Li(I)/Li(0) system.

Formation of a monolayer of magnesium on the tungsten substrate was not observed. This may be explained by the interfacial properties, i.e., wetting properties of the melt and the deposit with respect to the substrate. The co-deposition of lithium could be an important factor.

Formation of solid or liquid magnesium gives rise to different deposit shapes. When depositing solid magnesium, with eventually some dissolved liquid lithium, growth of Mg dendrites is clearly seen by different electrochemical techniques: cyclic voltammetry, chronopotentiometry and chronoamperometry. However, when depositing liquid magnesium, Li–Mg liquid solution is immediately formed, due to an increase in the UPD of Li. The metal droplets formed apparently coalesce easily due to the interfacial properties and a homogeneous deposit is obtained.

The diffusion coefficient of the Mg(II) species was determined by different electrochemical techniques (i.e., voltammetry, convolution analysis, chronopotentiometry and chronoamperometry). The values obtained showed that techniques using higher elapsed time give higher values of diffusion coefficient, which has been explained by the effect of increasing electrode area due to growth of the deposit, and/or by lithium co-deposition.

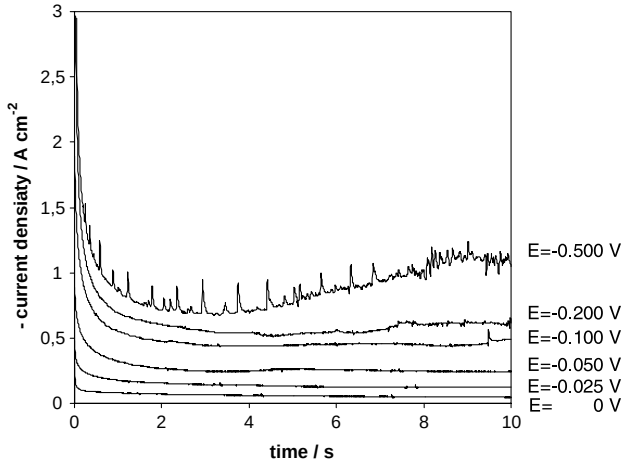

Fig. 13. Chronoamperograms obtained in molten eutectic LiCl–KCl mixture at 1000 K containing 2 mol% $MgCl_2$ Applied potentials vs Mg reference electrode.

Acknowledgements

The Research Council of Norway and Norsk Hydro ASA are acknowledged for financial support. A.M.M. wishes also to thank the 'Secretaría de Educación, Universidades, Investigación y Desarrollo' (Spain) for a post-doctoral grant. Mr. Oddmund Wallevik and Dr. Christian Rosenkilde, Norsk Hydro ASA, are acknowledged for fruitful discussions.

References

1. K. Andreassen, K.B. Stiansen and J.A. Jørgensen, Norwegian Patent 130119, 1974.
2. N. Høy-Petersen, T. Aune, T. Vrålstad, K. Andreassen, D. Øymo, T. Haugerød and O. Skåne, 'Ullmann's Encyclopedia of Industrial Chemistry', 5th edn, Vol. A15 (VCH, Weinheim, Germany, 1990), p. 559.
3. Kh.L. Strelets, 'Electrolytic Production of Magnesium', (Trans. by J. Schmorak, Keterpress Enterprises, Jerusalem, Israel, 1977).
4. S. Furihata, K. Akashi and S. Kurosawa, *Electrochim. Acta* **26** (1981) 1107.
5. K. Akashi, S. Furihata and S. Kurosawa, *Electrochim. Acta* **24** (1979) 581.
6. H.A. Laitinen and C.H. Liu, *J. Am. Chem. Soc.* **80** (1958) 1015.
7. E.N. Protasov, A.A. Gnilomedov and A.L. L'vov, *Elektrokhimiya* **14** (1978) 1296.
8. V.S. Tiunov, V.I. Mamaev and A.G. Morachevskii, *Fiz. Khim. Elektrokhim. Rasplavl. Tverd.* Elektrolitov, Tezisy Dokl. Vses. Konf. Fiz. Khim. Ionnykh Rasplavov Tverd. Elektrolitov 7th, **2** (1979) 122.
9. S. Le Vaguerese, CEA Report (1972) (CEA-R-4392), 67, *Nucl. Sci. Abstract* **27** (1973) 11743.
10. T. Støre, G.M. Haarberg and R. Tunold, *J. Appl. Electrochem.* **30** (2000) 1351.
11. G.S. Picard, F. Seon and B. Tremillon, *J. Electroanal. Chem.* **102** (1979) 65.

12. F. Seon, G.S. Picard, B. Tremillon and Y. Bertaud, French Patent 2514028, 1981.
13. N.G. Bukun and E.A. Ukshe, *Russ. J. Inorg. Chem.* **6** (1961) 465.
14. J.D. Van Norman and J.J. Egan, *P. Phys.Chem.* **67** (1963) 2460.
15. B. Børresen, 'Electrodeposition of magnesium from halide melts. Electrochemical kinetics and phase formation', Doctoral Thesis (NTH, Trondheim, Norway, 1995).
16. *in:* T.B. Massalski (Ed), 'Binary Alloys Phase Diagrams' 2nd edn (Materials Park, Ohio, 1990).
17. A.M. Martinez, B. Børresen, G.M. Haarberg, Y.Castrillejo and R.Tunold, *J. Electrochem. Soc.*
18. 'Thermochemical computer program FACTWin 3.05', Thermafact Ltd. Montreal, Canada.
19. B. Børresen, G.M. Haarberg, R. Tunold, G. Voyiatzis and G.N. Papatheodorou, Proceedings of the Jondal 2000 International Symposium on 'Spectroscopic and Electrochemical Studies of Formation of Dissolved Metal During Electrolysis in Chloride Melts', (Jondal, Norway, June 2000).
20. A.W. Adamson, 'Physical Chemistry of Surfaces', Chapter IX, 4th edn (John Wiley and Sons, 1982).